ACS APPLIED MATERIALS & INTERFACES

Research Article

www.acsami.org

Cross-linked Hybrid Nanofiltration Membrane with Antibiofouling Properties and Self-Assembled Layered Morphology

Ajay K. Singh, S. Prakash, Vaibhav Kulshrestha, and Vinod K. Shahi*

Electro-Membrane Processes Division, Central Salt & Marine Chemicals Research Institute, Council of Scientific & Industrial Research (CSIR), G. B. Marg, Bhavnagar-364002, Gujarat, India

Supporting Information

ABSTRACT: A new siloxane monomer, 3-(3-(diethoxy(2-(5-(4-(10-ethoxy-4-hydroxy-2,2-dimethyl-11-oxa-2-ammonio-6-aza-10-silatridecan-10-yl)phenyl)-1,3,4-oxadi azol-2-ylthio)ethyl)silyl)-propylamino)-2-hydroxy-N,N,N-trimethylpropan-1-aminium chloride (OA), was synthesized by reported 3-((4-(5-(2-((3-aminopropyl) diethoxysilyl)ethylthio)-1,3,4-oxadiazol-2-yl)-phenyl) diethoxysilyl)propan-1-amine (APDSMO) and glycidyl-trimethylammonium chloride (GDTMAC) by epoxide ring-opening reaction. OA-poly(vinyl alcohol) (PVA) hybrid antibiofouling nanofilter (NF) membranes were prepared by acid-catalyzed sol−gel followed by formal cross-linking. Membranes showed wormlike arrangement and self-assembled layered morphology with varying OA content. Hybrid NF membrane, especially OA-6, showed low surface roughness, high hydrophilic nature, low biofouling, high cross-linking density, thermal and mechanical stablility, solvent- and chlorine-tolerant nature, along with good permeability and salt rejection. Prepared OA-6 hybrid NF membrane can be used efficiently for desalting and purification of water with about 2.0 g/L salt content (groundwater in major part of India). The described method provides novel route for producing antibiofouling membranes of diversified applications.

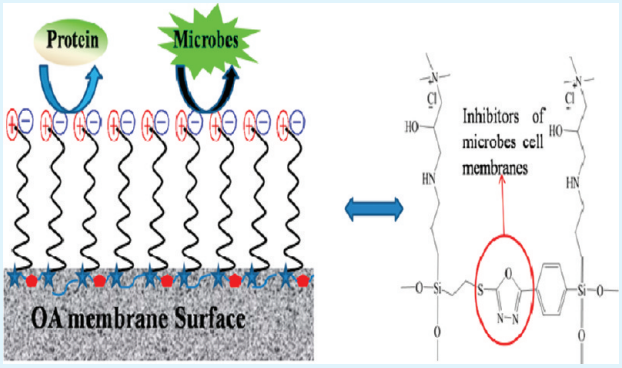

KEYWORDS: *1,3,4-oxadiazole, antibiofouling, sol−gel, nanofiltration, surface roughness, water purification*

1. INTRODUCTION

Desalination/purification of water is an urgent need in the 21st century for the regions where clean water supply is unavailable.[1] Membrane-based water treatment technologies, such as nanofiltration (NF) and reverse osmosis (RO), are energy efficient and suitable for easy integration as well as scale-up.[2] RO membrane contains a dense layer (ultrathin ≤0.1 μm) polymer active layer on top of porous support, while for NF membrane polymer active layer is porous (desecrate nanometer-size pores) and is usually charged.[3,4] NF membranes reject larger solutes (1−10 nm) via size exclusion, but partially reject monovalent ions. Thus, NF membranes are suitable for water desalination/purification of groundwater, when total dissolved solid (TDS) lies between 2000 and 3000 ppm for providing potable water with low TDS (>1000 ppm). Several polymer synthesis and surface modification strategies were explored to achieve nanoporous membrane.[5−7] NF membranes self-assembled morphologies of thin dense top layer and porous layer would be very attracting because of significant permeability and salt rejection. Organic−inorganic nanocomposite offered self-assembled and well ordered structure, which will be useful for developing NF membranes.[8]

Also, NF membrane should be chlorine tolerant, because sanitizing agents, especially chlorine,[9] is generally used for preventing bacteriological contamination of potable water. Generally, membranes (derived from either poly amide or poly(ether sulfone) are chemical instable in the presence of sanitizing agents, especially chlorine,[9] which is generally used for preventing bacteriological contamination of potable water. Numerous attempts have been made to develop chlorine tolerant membrane, based on hydrophilic modified poly(ether sulfone) (PES) including sulphonated PES.[10−12] However, decrease in permeate flux due to irreversible membrane fouling (organic fouling, colloidal fouling, and biofouling) is significant with these membranes. Among all types of fouling, formation of biofilm on the membrane surface (biofouling) is pervasive problem for material architecture.[13] Recently, surface modifications, such as epoxide coating,[14] amine coating,[15] graft polymerization,[16] noncovalent attachment,[17] and other covalently attached polymers,[18] were used to control membrane fouling. But, surface coating showed instability during chlorine treatment applications.[19−21] Furthermore, unprotected membrane is itself susceptible for biofouling, thus periodically chemical cleaning and disinfection are required to restore membrane performance.

Received: December 22, 2011
Accepted: February 23, 2012
Published: February 23, 2012

Biofouling is a pervasive problem during material designing for biomedical and water treatment devices. Autopsy studies of NF/RO fouled membranes revealed more than 50% of dry weight is of biological origin.[22] Thus, designing of chlorine tolerant antifouling membrane for water treatment pose the particular challenges because of its architecture (pore size, surface roughness and charged nature), along with chemical, mechanical, and hydraulic stabilities. Variety of polymers including polysiloxane and other silicon based materials, were used for health care[23] and biomedical product,[24−26] because of their cytotoxicity and desirable physical properties.[27] Organic/inorganic nanocomposites are generally organic polymer composites with inorganic nanoscale building blocks, which combine the advantages of the inorganic material (e.g., rigidity, thermal stability) and the organic polymer (e.g., flexibility, dielectric, ductility, and processability).[8,28−30] In addition, compounds bearing 1,3,4-oxadiazole ring showed antibacterial and antifungal activity.[31] Thus, there is great opportunity for developing organic−inorganic nanocomposite membranes, containing 1,3,4-oxadiazole and polysiloxanes, are expected to exhibit antimicrobial activity, membrane performance and stabilities.

In our previous study, we reported APDSMO siloxane monomer and prepared phosphonic acid grafted cross-linked antibiofouling membrane.[32] Herein, we are reporting a new silaxone monmer, 3-(3-(diethoxy(2-(5-(4-(10-ethoxy-4-hydroxy-2,2-dimethyl-11-oxa-2-ammonio-6-aza-10-silatridecan-10-yl)phenyl)-1,3,4-oxadi azol-2-ylthio)ethyl)silyl)-propylamino)-2-hydroxy-N,N,N-trimethylpropan-1-aminium chloride (OA), synthesized from APDSMO and glycidyltrimethylammonium chloride (GDTMAC) by epoxide ring-opening. Quaternary ammonium grafted and stable antibiofouling membranes with excellent flux and rejection were achieved by sol−gel followed by formal cross-linking. It was observed that membrane stabilities and performance were depend on degree of cross-linking because acetalization of oxidative sensitive primary alcohol groups (PVA) by formal reaction (cross-linking) lead to more stable ether-type linkages.

Also, performances of both types of membranes (MO-6 and OA-6) were compared in Table. 1. Bacterial zone of inhibition confirmed about 1.5 times high activity of OA in compare with APDSMO. Reported silaxone monomer (OA) showed 120 μg/mL MIC value, which is quite low in compare with APDSMO (3000 μg/mL).

Table 1. Comparative Filtration Performance of NF Membrane for Salt Solution at 25 °C

membrane	R_{NaCl} (%)	permeability (lm^{-2} h^{-1} bar^{-1})	ref
PCNFM3[a]	25.7	1.16	47
PECNM-2[a]	24.2	1.4	48
GCTACC/PAN[b]	36.0	1.43	49
NF-7[a]	37.6	3.55	50
MO-6[a]	55.4	5.77	32
OA-6[b]	68.31 ± 0.01	1.24 ± 0.01	this work

[a]1 g L^{-1} NaCl solution. [b]2 g L^{-1} NaCl solution.

2. EXPERIMENTAL SECTION

2.1. Materials. Aminopropyltriethoxysilane (APTEOS) (99%), glycidyltrimethylammonium chloride, and polyethylene glycol (PEG) (different molecular weights) were obtained from Sigma-Aldrich Chemicals. Poly(vinyl alcohol) (M_w: 125 000), formaldehyde (37% in water), phosphorous acid, hydrochloric acid, sulphuric acid, *p*-chloro benzoic acid, hydrazine hydrate, carbon disulfide, sodium hydroxide, sodium chloride, sucrose, magnesium chloride, sodium hypochlorite, *N*-methyl pyrrolidone, dimethylformamide, hexane, iodine crystal, magnesium turnings, tetrahydrofuran (THF), streptomycin, fluconazole, acetone, and methanol were obtained from S.d. fine chemicals, Mumbai, India. Solvents were used after proper distillation, and Milli-Q water was used for all experiments.

2.2. Synthesis of Silica Precursor. Synthesis of 2-(2-chloroethylthio)-5-(4-chlorophenyl)-1,3,4-oxadiazole has been described in Section S1 in the Supporting Information. Methodology used and reaction scheme for synthesis of 2-(2-aminopropyldiethoxysilaneethylthio)-5-(4-aminopropyldiethoxy silanephenyl)-1,3,4-oxadiazole (APDSMO) are described in the Supporting Information (Section S2 and Scheme S1, in the Supporting Information). Silica precursor (3-(3-(diethoxy(2-(5-(4-(10-ethoxy-4-hydroxy-2,2-dimethyl-11-oxa-2-ammonio-6-aza-10-silatridecan-10-yl)phenyl)-1,3,4-oxadiazol-2-ylthio)ethyl)silyl)propylamino)-2-hydroxy-N,N,N-trimethylpropan-1-aminium chloride) (OA) was synthesized by epoxide ring-opening reaction (Scheme 1) and proposed mechanism has been included in Scheme S2 in the Supporting Information.[33] In a typical synthetic procedure, 1:1 mol ratios of APDSMO and GDTMAC, were stirred at 80 °C for 6 h. Thus obtained yellowish colored transparent liquid of OA was obtained, which structure was confirmed by FTIR, ^{1}H NMR, ^{13}C NMR, and elemental analysis.

Scheme 1. Preparation Route for Silica Precursor (OA), and Hybrid NF Membranes

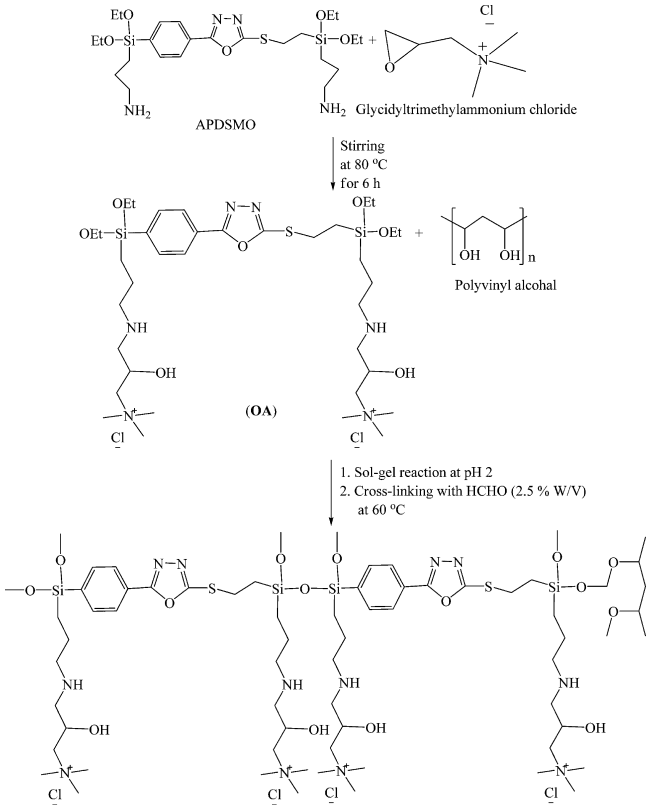

Yield: 80% (yellow colored transparent liquid). IR cm^{-1}: 3401 (−OH), 2979 ($-CH_3$) 2935, 1638, 1481 (quaternary ammonium chloride), 1600 (C═N oxadiazole), 1551 (NH), 1285 (N−N), 1115 (C−O−C oxadiazole), 1048 ($-OCH_2CH_3$) 1013 (Si−O−C), 781 (C−Si), 693 (Si-Ph); ^{1}H NMR (D_2O): δ 7.74 (Ph-Si), 7.37 (Ph-Oxadiazole), 4.45,4.27 (−CH−OH), 3.47 (−OH), 3.44 ($-CH_2-NMe_3$) 3.39, 3.29 ($-OCH_2CH_3$, $-SCH_2CH_2$), 3.10 (Me_3N), 2.86

(−CH_2−NH−CH_2−), 2.57 (−CH_2−CH_2−Si-) 1.51, (−NH, −CH_2Si), 0.57 (−CH_2Si); ^{13}C NMR (DMSO-d_6):δ 168.4,166.0,136.5,135.2,130.6,128.4,73.2,68.9,68.1, 66.3,64.4,63.6,58.3,57.5,54.2,52.1,41.8,22.0,21.7,19.1,10.1,9.; Anal. Calcd for [$C_{24}H_{44}N_4O_5SSi_2$] (858.41): C, 50.27; H, 8.44; N, 9.77; S, 3.73, Si, 6.53. Found: C, 50.24; H, 8.4; N, 9.77; S, 3.70, Si, 6.52.

2.3. Membrane Preparation. OA-PVA hybrid nanofiltration membranes (NFMs) were prepared by acid catalyzed sol−gel followed by formal cross-linking (Scheme 1). Desired amount OA was added to PVA solution (10 wt % dissolved distilled water under stirred conditions) and mixture was stirred constantly for 6 h. Obtained solution was transformed into viscous white colored gel by adding 2 mL HCl (1M) under constant stirring (6 h) at room temperature. Resultant gel was transformed as thin film on glass plate, with help of doctor blade. Thin film was allowed to dry under room temperature (10 min) and precipitated in hexane at 10 °C for 20 min, obtained membranes were dried at 30 °C for 24 h, followed by at under vacuum oven at 80 °C (24 h). Dried membranes were subjected to formal cross-linking in HCHO(2.5% w/v) + H_2SO_4 at 60 °C for 3 h.[34] Cross-linked membrane was washed thoroughly by double distilled water followed by in 1.0 M HCl and NaOH solutions, successively. Conditioned membranes were converted into Cl^- form by equilibrating in 1.0 M NaCl solution for 12 h. The equilibrated membrane was stored in doubled-distilled water for further characterizations. Different prepared membranes were designated as OA-X, where X is the (weight percentage of OA)/10 in the membrane phase. Details for instrumental analysis can be found in Section S3 in the Supporting Information.

2.4. Membrane Flux, Rejection, Contact Angle, and Pore Radius Measurements. Membrane discs (2.0 cm radius and 100 ± 10 μm thickness) were soaked in water for 15 min prior to filtration. Latter, it was assembled in a two compartments stainless steel cell (effective membrane 12.56 cm^2) equipped with stirrer and designed for dead-end filtration. Deionized water with (18 mΩ cm^{-1} resistivity) was initially passed through the membrane with 12 bar pressure at ambient temperature (25 °C) until steady-state flux was obtained. Aqueous solutions of PEG with different molecular weights (2000 ppm; prefiltered through 0.45 μm syringe filters) were used to measure the membrane flux and rejection. The first 5 mL of permeate was discarded, and percent rejection was obtained from permeate concentration (constant value). Membrane permeability and rejection was estimated by permeate and feed concentration using following equations.[35] All experiments were carried thrice and average values were used.

$$\text{permeability (L m}^{-2}\,\text{h}^{-1}\,\text{bar}^{-1}) = \frac{\text{permeate volume (L)}}{\text{membrane area (m}^2) \times \text{time (h)} \times \text{applied pressure (bar)}} \quad (1)$$

$$\text{rejection (\%)} = \left[1 - \frac{\text{permeate concentration}}{\text{feed concentration}}\right] \times 100 \quad (2)$$

For the estimation of effective pore size of the membranes, Ferry equation (eq 3) was used to correlate the rejection of spherical solutes by the membrane, considering uniform pore size distributions.[36]

$$R = 100 \times [1 - (1 - r/a)^2]^2 \quad (3)$$

Where R is the percent rejection, r is the solute diameter, and a is the pore size (diameter) of the membrane (assuming a uniform pore size) and can be obtained by: $r = 2b$. The stokes radius b can defined by

$$b = 16.73 \times 10^{-10} M^{0.557} \quad (4)$$

M is molecular weight of solute (g/mol). Obtained rejection data was fitted in Ferry equation (Figure S1 in the Supporting Information) and molecular weight cutoff rejection data for neutral probe pore diameter was estimated. Static water contact angles for prepared membranes were measured by the sessile drop method with contact angle goniometer equipped with video camera and image analysis system.

2.5. Membrane Stabilities. Chemical stability of prepared membranes was analyzed for different solvents in term of weight loss by following equation.

$$W_l = \left[1 - \frac{W_{dry}}{W_s}\right]100 \quad (5)$$

Where W_{dry} and W_s are the weight of dry and chemically treated dry membrane.

Membrane chlorine stability (0.5−5 g/L) was analyzed under sodium hypochlorite solution (free chlorine content of 14 wt %) for different time (0−72 h) interval at 80 °C. Membrane stability was evaluated in terms of weight loss (eq 5), and change in flux/rejection performance.

2.6. Antifungal and Antibacterial Activity. One ml of OA (silica precursor) aqueous solution (3000, 1000, 100, 10 μg/mL) was added with 9 mL of nutrient agar medium in presterilized petridishes under constant dish rotation for homogeneous mixing. Then, fungus or bacterial strains were inoculated in dishes (diameter 5 mm) and growth of inhibition was measured by eq 6.

$$\%\ \text{growth inhibition} = \left[1 - \frac{t_d}{c_d}\right]100 \quad (6)$$

Where c_d is the colony diameter of treated set and t_d is colony diameter of control set.

The minimum inhibitory concentration to kill 90% of bacterial population (minimum inhibitory concentration (MIC)) for *E. coli* and *B. Subtilis* was determined by reported method.[37] Bacteria were grown overnight in 10 mL of Luria Base (LB media) at 37 °C and 220 rpm. 100 μL of overnight culture was subcultured in 10 mL of LB under similar conditions. Obtained bacterial solution showed 2.2299 OD_{600}. One ml of this solution was then inoculated into LB broth containing various concentrations of OA (silica precursor) for maintain OD_{600} at 1.000 by adding sterilized water. Cultures were then grown in above-mentioned conditions and bacterial growth was determined by measuring OD_{600}. For membranes, preweighed sample was dipped in 10 mL of *E. coli* containing LB broth (OD_{600} = 1.000), while one control set was used for reference growth. For determining bacteriostatic or bactericidal nature of silica precursor (OA) or membranes, their different amount (10−10000 μg/mL) were incubated with *bacteria* in aqueous LB broth for 24 h. One-hundred milliliter aliquots withdrawn from incubated LB broth and placed on nutrient soft agar plates under growing conditions, for colony counting.

3. RESULTS AND DISCUSSION

3.1. Preparation of Nanocomposite Membrane. Monomer (APDSMO) was synthesized by Barbier−Grignard reaction using dichloride of 2-(2-chloroethylthio)-5-(4-chlorophenyl)-1,3,4-oxadiazole and APTEOS, see Scheme S1 in the Supporting Information. 2-(2-Chloroethylthio)-5-(4-chlorophenyl)-1,3,4-oxadiazole is an inexpensive antimicrobial compound and procedure for its synthesis has been included in Scheme S1 in the Supporting Information. Synthesized compound was confirmed by the ^{1}H NMR and ^{13}C NMR spectra (Figure S2−S8 in the Supporting Information). Silica precursor OA was synthesized via epoxide ring-opening with −NH_2 group (Scheme 1) (see Scheme S2 in the Supporting Information). APDSMO contains amine group and behaves like nucleophile (lone pair electron of nitrogen shifts toward epoxide ring and forms intermediate compound and finally converts into secondary alcohol). ^{1}H NMR spectra of OA (see Figure S7 in the Supporting Information) exhibited shift at 0.509 ppm for Si−CH_2− protons. Shifts at 1.514 and 3.473 ppm were designated to −NH and secondary −OH. Different methylene protons were observed at 2.864, 2.574 ppm. Chemical shifts at 3.296, 3.101 ppm were assigned to

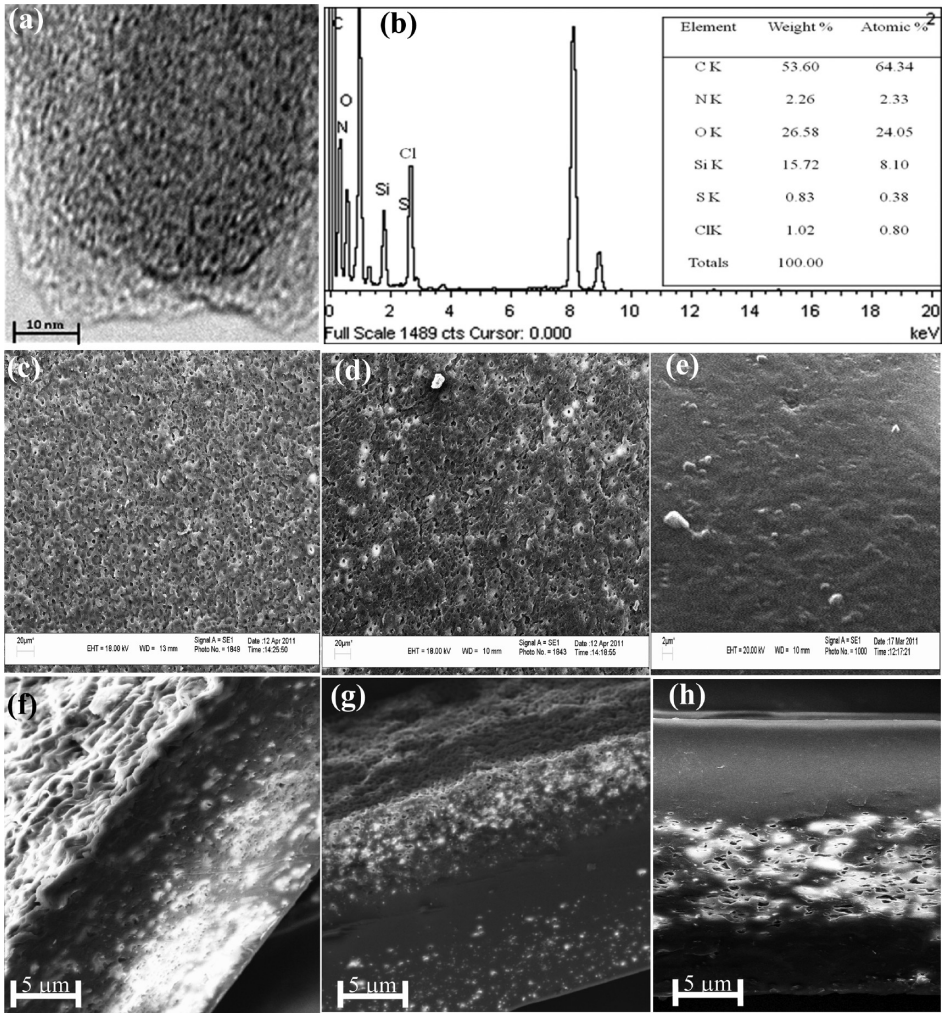

Figure 1. (a, b) Microscopic characterization (TEM and EDX) for OA-6 membrane; (c–e) SEM images (surface view) for OA-3, OA-4, and OA-6 membranes, respectively; (f–h) SEM images (cross-section) for OA-3, OA-4, and OA-6 membranes, respectively.

$-N^{+}(CH_3)_3$, while at 3.339 ppm was attributed to $-OCH_2CH_3$ protons. In ^{13}C NMR spectra (see Figure S8 in the Supporting Information), peaks at 9.780, and 10.142 ppm were assigned as to $-Si-CH_2-$ and $Ph-Si-CH_2-$ carbons respectively, while for oxadiazole ring, carbons shifts were obtained as 168.402 and 166.002 ppm. In silica precursor (OA), presence of phenyl was confirmed by shifts at 136.514, 135.282, 130.655, and 128.429 ppm. Peaks at 52.110 and 54.200 ppm were attributed to quaternary ammonium carbons. Another carbon peak of different methylene group and secondary alcohol carbons was described in ^{13}C NMR spectra, see Figure S8 in the Supporting Information.

FTIR and ATR spectra of APDSMO, OA and OA-6 membrane, were included in Figure S9 & S10 in the Supporting Inforamtion. Presence of oxadiazole ring in APDSMO and OA was confirmed by the strong intensity band at 1092 and 1115 cm^{-1} (C–O–C stretching vibration).[38] APDSMO showed two medium intensity bands at 3350–3400 cm^{-1} and 1549 cm^{-1} ν(N–H) and a medium intensity band at *ca.* 1590 cm^{-1} ν(C═N) of oxadiazole ring.[38] For OA (silica precursor), stretching vibrations at 2935, 1638, and 1480 cm^{-1} were assigned to the quaternary ammonium groups.[34] while stretching vibration at 2979, 1048 cm^{-1} were assigned to $-CH_3$ groups (asymmetric vibration and (–O–Si–O- stretching vibrations).[39] Membrane forming material was prepared by acid catalyzed sol–gel and condensation polymerization of OA and PVA in aqueous media. Obtained transparent thin film was cross-linked by formal reaction (two steps process) for 3 h at 60 °C. Formaldehyde reacted with –OH group (PVA) and formed hemiacetal, which further reacted and resulted acetal formation. Due to cross-linking, membrane lost transparency in wet conditions, while it was retained in dry state. ATR-FTIR spectra of cross-linked OA membranes (Figure S10 in the Supporting Information) showed absorption band at −3439 cm^{-1}, which was attributed to –OH stretching vibration, while, at 2920 cm^{-1} to $-CH_2$ stretching vibration. Weak absorption band at 1487 cm^{-1}, corresponds to $-OCH_2$ deformation and wagging vibration. Peak at 1637 and 3309 cm^{-1} confirmed the presence of quaternary ammonium group and salt, respectively.[34] Cross-linked structure of membrane was confirmed by cyclodiether (–C–O–C–) due to peak at 1017 cm^{-1}.[34] The absorption band at 1133 cm^{-1} (characteristic Si–O–Si asymmetric stretching and Si–O–C) confirms molecular level of hybridization between organic and inorganic segments. Under acidic condition, PVA reacted with cross-linking agent (formaldehyde) and silanol groups and resulted formation of C–O–C (1384 cm^{-1}) and Si–O–C groups, which favored better compatibility between organic and inorganic segments, homogeneous molecular level silica distribution in the membrane phase. On the basis of these studies, schematic

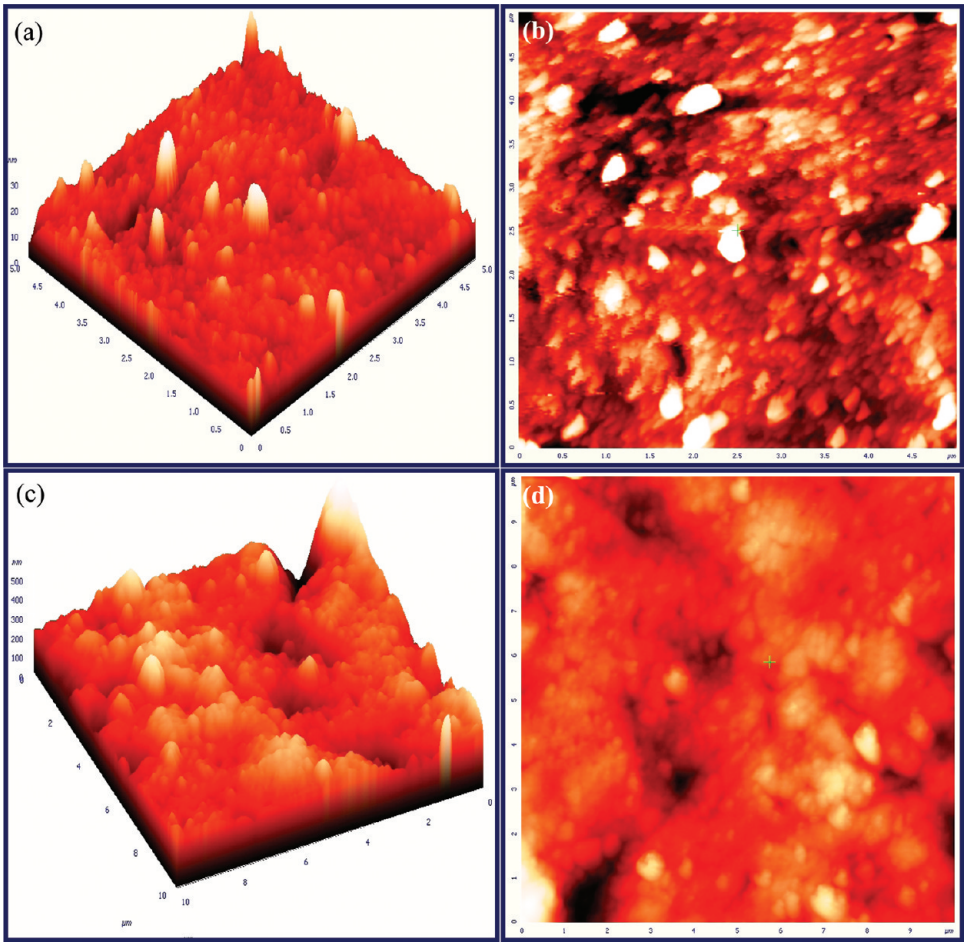

Figure 2. AFM images of NF membranes; (a, b) OA-6; and (c, d) OA-5.

structure of organic−inorganic hybrid NF membrane is depicted in Scheme 1.

3.2. Surface Morphology of Membranes. TEM images and EDX analysis data for hybrid cross-linked membranes, revealed homogeneous silica distribution in membrane matrix (Figure 1(a,b)). Relatively large quaternary groups with worm like arrangement in the matrix were created for membranes with high organic content (PVA). 50 N m fine slices of membrane were obtained by microtome and HRTEM image analysis confirmed the absence of crystalline silica (membrane lattice finges are absent in 1−10 nm range). In our previous study, MO membranes showed crystalline silica with clear lattice finges.[32] In this case (OA membrane), absence of crystalline silica confirmed the reducing properties of phosphoric acid, responsible for good mechanical stability of membranes. Amorphous nature silica in membrane matrix was further confirmed by WXRD data; see Figure S11 in the Supporting Information. SEM images for different hybrid OA-X membranes (Figure 1(c−e) and Figure S12 in the Supporting Information), showed that membrane have regular arrangements and with increasing silica content in membrane matrix self-architecture porous and dense layer was obtained. Membrane turned to dense with increase in OA content, may be due to increased cross-linking density (high storage modulus) and favorable Si−O−C and Si−O−Si bond formation. For high OA content in membrane matrix (OA-6), layered morphology was observed. Surface roughness of membranes play important role in filtration. Low surface roughness (smooth surface) of membrane is favorable to avoid the fouling. Membrane surface roughness was studied by AFM, and images confirmed polycondensation of APDSMO, and thus conglomeration in membrane matrix (Figure 2(a−d)). Surface roughness measurements showed that un-cross-linked (pristine) membrane exhibited lowest roughness (0.043 μm), whereas surface roughness for OA-3, OA-4, and OA-6 hybrid membranes were observed as 0.287 nm, 0.117 nm, and 0.053 μm, respectively. All data are average of triplicate measurements for 1.4 × 1.4 μm^2 membrane surface area with ±0.005 μm of maximum error. Quite smooth surface and self-assembled layered morphology of these hybrid membranes are attractive features, which controls membrane permeability and salt rejection.

3.3. Thermal, Mechanical, and Chemical Stabilities. TGA curves for representative hybrid membranes (see Figure S13 in the Supporting Information), showed two steps weight loss. In the first step, membrane lost absorbed water, whereas in the second step, degradation of quaternary ammonium group and membrane matrix occurred.[40] Rate of water loss decreased with OA content because of the increase in hydrophilic functional groups. Beyond 290 °C, rapid decomposition of membrane samples completed up to 460 °C. Maximum char of initial weight (8.65%) was left out in the OA-6 membrane, which may be due to the formation of silica cluster. Functionalization at inorganic part (silica) and cross-linking improved membrane thermal stabilities.

First endothermic peak (T_g value) for OA-3, OA-4, and OA-6 membranes was recorded as 83.87, 90.39, and 112.16, respectively, from DSC thermograms, see Figure S14 in the Supporting Information. Incorporation of silica precursor in organic matrix had a profound effect on T_g value, which increased with silica content. T_g value of pristine PVA membrane was found to be 78 °C.[41] These observations may be explained by the plasticizing effect and degree of cross-linking. The dynamic mechanical analysis for different hybrid membrane at 10 N applied force and 1 Hz (see Figure S15 in the Supporting Information), indicated increase in young modulus with silica content because formation of continuous network within organic polymer due to cross-linking. Cross-linking density of membrane (ρ) was determined by following equation.

$$\rho = \frac{E'}{3d\varphi RT} \quad (7)$$

Where d is the membrane density, f is the front factor (where $f = 1$), R is universal gas constant, and T is absolute temperature. The young modulus, E', was determined by dynamic mechanical analyzer under 10 Hz frequency at varied temperature (30−320 °C). For different hybrid NF membranes, young modulus and cross-linking density increased with silica content (see Figure S16 in the Supporting Information). These variations may be explained by formation of cohesive domains between organic and silica. Thus it is necessary to optimize the silica precursor (OA) content in the membrane matrix for achieving better mechanically stable hybrid membranes.

Generally, sodium hypochlorite is being used for removing of microbes (disinfectant) from municipal water, and its strong oxidizing nature jeopardized membrane integrity under operating conditions. Thus, membrane chlorine tolerant nature was accessed in terms of weight loss after treating the membrane in 5% NaOCl solution(aq) for different time intervals (0−72 h) (Figure S17, see the Supporting Information). For hybrid membrane, weight loss increased with silica content, because increase in quaternary ammonium group in membrane matrix. Moreover, no appreciable weight loss was exhibited by membranes after 25 h treatment. Membrane stability in different organic solvent was checked and obtained results a re presented in Table S2 in the Supporting Information. Membranes have chemically inert silica and acetylated PVA, which is also chemically stable, and therefore membranes were undissolved in tested organic solvents.

3.4. Nanofilteration Performance. Permeability of hybrid NF membranes was evaluated for different solvents in, and varied as: water > DMF > methanol > acetone, in similar fashion to the dielectric constant (see Figure S17 in the Supporting Information). Also, membrane permeability decreased with silica content (OA) in the membrane matrix, which may be attributed to relatively high extent of cross-linking for high silica content (low PVA content). Membrane flux data for different solvents measurements confirms that high membrane permeability in polar solvents and low permeability in nonpolar solvent. Feed water pH was varied from 1 to 12 and received data was systematized in Figure 3a and ensure that membrane OA-6 water permeability minimum differentiating while OA-3 membrane water permeability varied with pH.

Membrane permeability and solute rejection performance (NaCl, $MgCl_2$, poly(ethylene glycol), and sucrose; 2000 ppm)

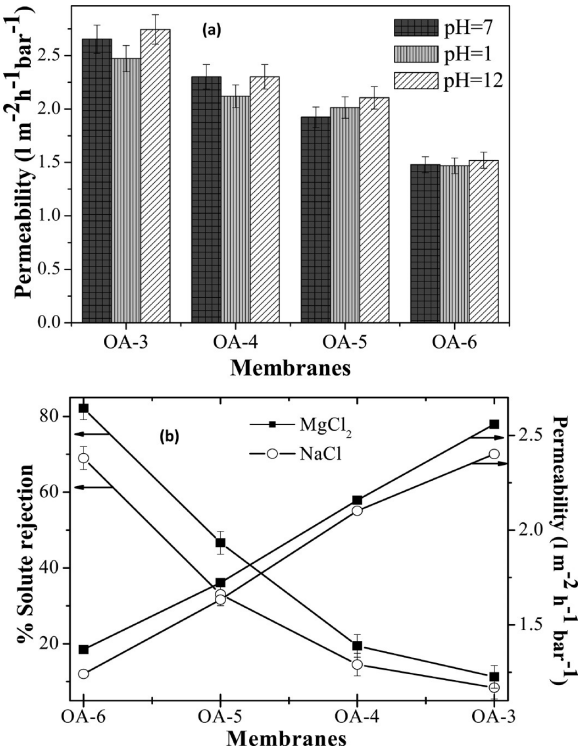

Figure 3. (a) Membrane permeability at different pH; (b) solute permeability and rejection for NaCl and $MgCl_2$ (feed solution concentration 2 g/L, 11 bar applied pressure, 30° temperature) (maximum error for permeability ±0.01 L m^{-2} h^{-1} bar^{-1} and solute rejection was ±0.01%).

are presented in Figure S18 in the Supporting Information. Variation of membrane permeability and salt rejection for NaCl and $MgCl_2$ solutions (2.0 g/L) at constant applied pressure (11 bar) showed membrane permeability decreased with increase in OA content (silica precursor) in the membrane matrix, and OA-6 membrane exhibited 1.24 and 1.37 L m^{-2} h^{-1} bar^{-1} permeability for NaCl and $MgCl_2$ solution, respectively (Figure 3(b)). As a reference, OA-3 membrane showed 2.40 and 2.56 L m^{-2} h^{-1} bar^{-1} permeability for NaCl and $MgCl_2$ solution, respectively. Low flux for NaCl solution may be attributed to high osmotic pressure, which depends on the van't Hoff factor, and molecular weight of solute. Salt rejection values under similar experimental conditions showed the opposite trend and OA-6 membrane showed 69.01 and 82.13% salt rejection for NaCl and $MgCl_2$ solutions, respectively (Figure 3b). Thus, lowest permeability and highest salt rejection values were showed by OA- 6. These data will help us to tailor desired type of hybrid NF membranes. Prepared hybrid NF membrane showed self-assembled layered morphology, which is responsible for membrane permeability and salt rejection.

Molecular weight cutoff (MWCO) for different hybrid NF membranes was estimated by probe solutes (PEG with 200−10 000 Da MW). MWCO was considered as molecular weight of PEG exhibited more than 90% rejection. Molecular weight cutoff data for different NF membrane was expressed in Figure 4a and Table S1 in the Supporting Information. On the basis of neutral probe solute rejection data, membranes pore diameter were estimated with help of Ferry equation, which described the percent rejection (R) expected for a membrane with uniform circular pores of diameter (a) as a function of the diameter of spherical solutes (r).[42] Molecular/ionic size for

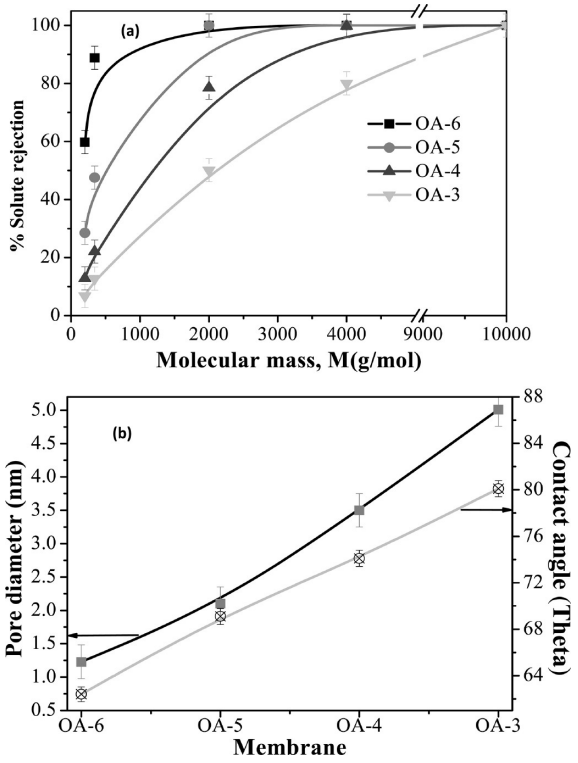

Figure 4. (a) Solute rejection of PEG (different molecular weights) (maximum error for solute rejection ±0.01%); (b) pore diameter and contact angle of membrane with varied silica content (maximum error for pore diameter ±0.01 nm and contact angle ±0.1θ).

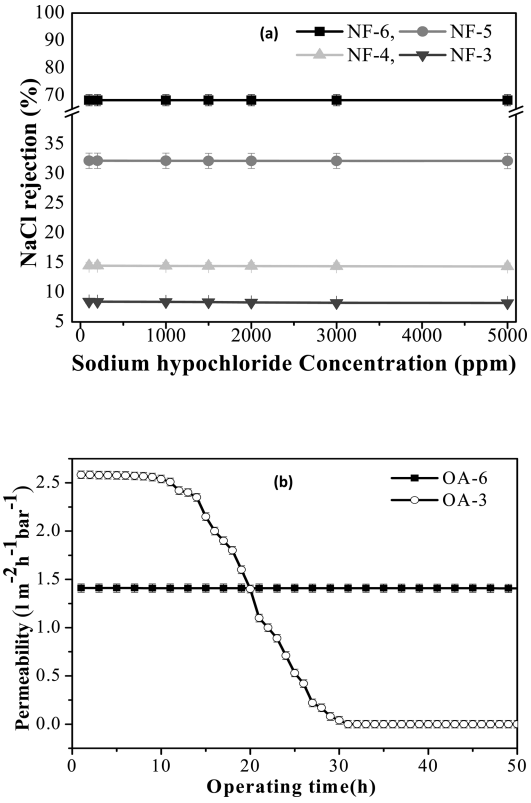

Figure 5. Short-term stability test; (a) effect on salt rejection after treatment with NaOCl solutions (100−5000 ppm) (maximum error for rejection was ±0.01%); (b) microbial stability test; conditions employed: LB media; feed solution 1.00 ± 0.01 OD at 600 nm; pressure 11 bar; and temperature 25 °C (,aximum error for permeability was ±0.01 L m^{-2} h^{-1} bar^{-1}).

neutral or ionic probes were obtained from literature.[43,44] Hydrophilic/hydrophobic, charged and surface roughness of the membrane surfaces are important considerations for its antifouling properties.[45,46] Membrane contact angle data were used to elucidate its hydrophilic/hydrophobic characteristics. Membrane contact angle and pore diameter, both decreased with increase in silica precursor (OA) content in the membrane matrix (Figure 4b). Silica plays important role to control hydrophilic nature. Further, hybrid NF membranes with 1.23−5.01 nm pore diameter, are suitable for water purification/desalination.

Chlorine tolerance nature of these silica derived membranes was studied after exposure of membrane in NaOCl solutions (0.0−5.0 g/L). Salt rejection values for 2.0 g/L NaCl feed solution of different membrane after 24 h exposure in different NaOCl solutions, revealed that membrane filtration performance was unaffected (Figure 5a). The chlorine stability of these PVA based cross-linked membranes may be attributed to the formation of highly stable ether type of linkages due acetylation of oxidative sensitive primary alcohol groups (PVA) by formaldehyde.[19] Formal cross-linking reaction can be both intra- and intermolecular, and high amount of formaldehyde used in cross-linking would sure that PVA is essentially quantitative. This type of membrane will be most useful for the future desalination and industrial application.

Prepared NF membrane (OA-6) showed 68.31% salt rejection value (Table 1), which is higher than that for previously reported membrane (MO-6) by our research group.[32] Thus, reported OA-6 hybrid NF membrane can be used efficiently for desalting and purification of water with about 2.0 g/L salt content. In most part India, groundwater salinity varied between 2.0 and 4.0 g/L, and reported OA-6 hybrid membrane is highly useful for providing safe water for habitants. Effect of biofouling using *Escherichia coli* bacteria (grown bacterial solution of OD_{600} = 1.0 ± 0.1 for 24 h) was studied by membrane permeability values for different operating time, 2−50 h, obtained results systematized in Figure 5b. Results revealed that OA-3 membrane (low OA content) lost complete permeability after about 10 h operation, whereas OA-6 (high OA content) membrane did not showed any deterioration in permeability after 50 h operation. Thus, OA-6 membrane can be utilized with advantage without biofouling for nanofiltration in aqueous media. Although, mechanism for biofouling control on the membrane surface is still uncertain but terminal quaternary ammonium groups and long carbon chain of the silaxone monomer (OA), might have behaved like a brush to avoid the microbes attachments on the membrane surface. In the case of accumulated microbes on the membrane surface, 1,3,4-oxadiazole ring acted as a drugs and destroy them. These phenomena might have been responsible for for antimicrobial activity of the membranes.

3.5. Antimicrobial Studies. In this study, two bacterium (*E. coli, B. subtilis*) and one fungus (A. niger) were used for antibiofouling performance. Antifungal activity of silica precursor and hybrid NF membranes was studied and fungal growth of inhibition data at different concentrations (10, 100, and 300 μg/mL) was showed in Figure 6a−c and obtained results were systematized in Table 2. Silica precursor (OA) showed antifungal activity and complete growth inhibition at 300 μg/mL concentration. Antibacterial activity for OA and

dx.doi.org/10.1021/am201821a | ACS Appl. Mater. Interfaces 2012, 4, 1683−1692

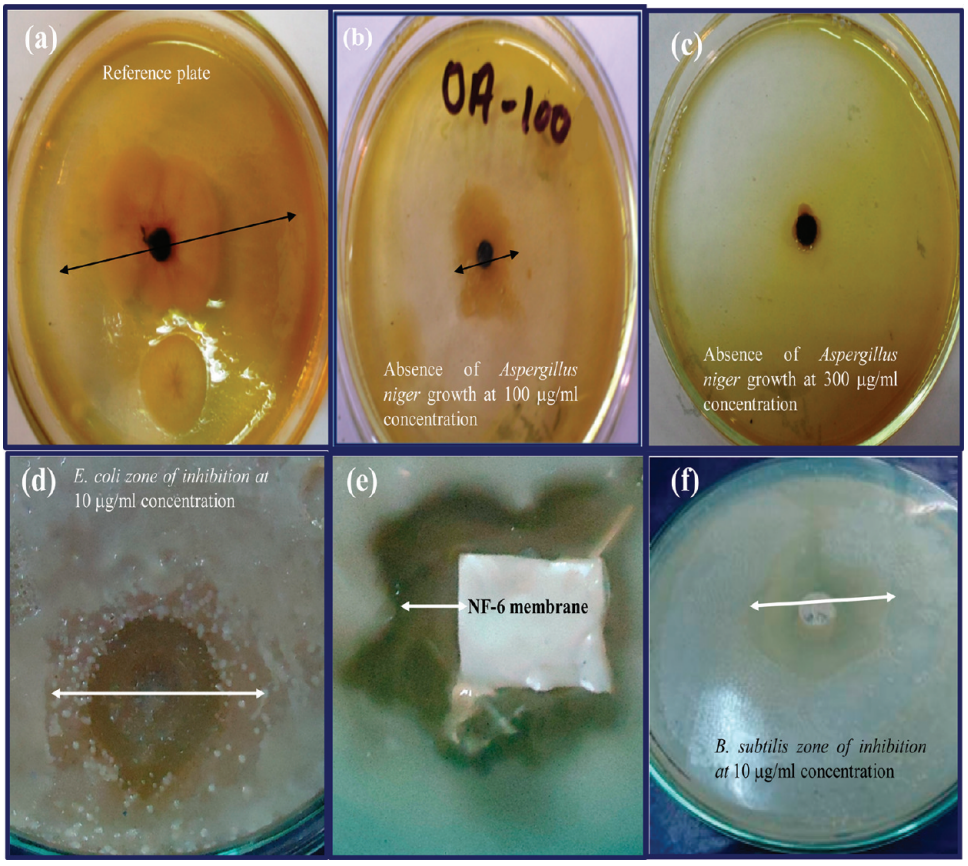

Figure 6. Digital picture of (a) control set without adding any drug; (b) silica precursor at 100 μg/mL concentration; (c) silica precursor at concentration 300 μg/mL; (d) *E. coli* zone at concentration 10 μg/mL; (e) OA-6 membrane *E. coli* zone; (f) *B. subtilis* zone at 10 μg/mL concentration.

Table 2. Antimicrobial Activity of Silica Precursor (OA), NF Membranes and Standard Drugs

	bacterial zone of inhibition (mm)		% inhibition of *A. niger* at conc. (μg/mL)		
compd	*E. coli* Gram −ve	*B. Subtilis* Gram +ve	10	100	300
OA	$18^a \pm 1$	$20^a \pm 1$	37 ± 1	73 ± 1	100 ± 1
OA-6	$6^b \pm 0.5$	$7^b \pm 0.5$			
OA-5	$5^b \pm 0.5$	$6^b \pm 0.5$			
OA-4	$3^b \pm 0.1$	$4^b \pm 0.1$			
Streptomycin	$22^a \pm 1$	$24^a \pm 1$			
Fluconazole			100 ± 1	100 ± 1	100 ± 1

[a]Represent at 10 μg/mL concentration. [b]Represent 100 mg weight of membrane.

membrane was studied in terms of zone of inhibition and MIC value. Relevant digital images are presented in Figure 6d−f and data are included in Table 2. Bacterial zone of inhibition was measured by well-forming methods, 5 mL of hard agar was dispersed in petriplates ,and after 10 min, 5 mL of soft agar was placed in petripaltes. After 30 min, 1 mL of Gram +ve bacterium (*B. subtilis*) or Gram −ve bacterium (*E. coli*) dispersed in petriplates.[32] After formation of a well by a sterilized tip, 1 mL of silica precursor (OA) (10 μg/mL) was added to each well for bacterium grown under appropriate conditions; after 24 h, bacterial zones were measured. Prepared silica precursor was more active against Gram +ve bacterium *B. subtilis*. In case of membrane, 100 mg UV-sterilized membrane was pasted on soft agar surface, and the above-mentioned procedure was followed. Bacterial zone of inhibition confirmed about 1.5 times high activity of OA in comparison with APDSMO.

MIC values for silica precursor and hybrid membranes are included in Table 2. Comparative study of MIC data for silica monomer previously reported and synthesized silica precursor (organosiloxane) systematized in Table 3. Reported silaxone monomer (OA) showed 120 μg/mL MIC value, which is quite low in compare with APDSMO (3000 μg/mL).[32] The mechanism for the increments of microbial activity was unknown but High solubility, particle size, lipophilicity, and dipole moments of OA may be the main factors for its quite low MIC value and thus enhanced microbial activity.

4. CONCLUSIONS

In our previous study, a siloxane monomer (APDSMO) with good antimicrobial properties was reported. But, APDSMO was easily hydrolyzed in atmosphere and formed polysiloxane, which affected its antimicrobial properties. Now, we are reporting the synthesis of new monomer precursor (OA) by

Table 3. Comparative Antibacterial Properties for Synthesized Silica Precursor (OA) and Other Reported Compounds

compds	MIC (μg/mL) *Escherichia coli*	MIC (μg/mL) *Bacillus subtilis*	ref
oligosilesquixane	160		51
polysilsesquixane	2500		52
penicilline	256		52
siloxane	80		52
MO	3000		32
OA	120 ± 10	70 ± 3	this work

APDSMO and glycidyltrimethylammonium chloride, epoxide ring-opening reaction. Hybrid NF membranes with different silica precursor (OA) content were prepared by acid catalyzed sol−gel followed by formal cross-linking. Based on spectroscopy studies, schematic structure of hybrid membrane was proposed. Hybrid NF membrane, especially OA-6, showed low surface roughness, hydrophilic nature, lower biofouling, higher cross-linking density, stability (thermal, mechanical, and solvents), and chlorine tolerant nature. Wormlike arrangement in the membrane matrix with silica precursor (OA) content and self-assembled layered morphology of these hybrid membranes are attractive features, which controls membrane permeability and salt rejection. Pore diameter (1.23−5.01 nm), chemical stability, antibiofouling, chlorine tolerance and antimicrobial nature of synthesized membrane suggested their suitability for water desalination/purification. Performance of different prepared membranes were compared with reported membrane in the literature, this suggest potentiality of prepared hybrid membrane, especially OA-6, for high flux and salt rejection.

Antimicrobial properties of hybrid membranes were tested against waterborne fungi (*Aspergillum niger*) and coliform bacteria (*Escherichia coli*), and OA-6 membrane (high OA content) exhibited good antimicrobial properties to avoid the biofilm formation on membrane surface and thus any deterioration in performance. Comparative study of our previous work concludes that quaternary ammonium terminated surface is more microbial active than phosphonic acid group.

Further studies are aimed to optimize the polymer structure and architecture, for still best membrane permeability, solute rejection, and antibiofouling properties. Detailed study on structural parameters, long-term durability, degree of cross-linking, and functional group density are necessary to develop water borne polymer with antimicrobial membrane for water purifications.

■ ASSOCIATED CONTENT

Supporting Information

The details of siloxane preparation, spectral analysis, chlorine tolerance, WXRD, present as sections S1−S3, Scheme S1, Figures S1−S19, and Table S1 and S2. This material is available free of charge via the Internet at http://pubs.acs.org/.

■ AUTHOR INFORMATION

Corresponding Author

*Tel: +91-278-2569445. Fax: +91-278-2567562/2566970. E-mail: vkshahi@csmcri.org or vinodshahi1@yahoo.com.

Notes

The authors declare no competing financial interest.

■ ACKNOWLEDGMENTS

Instrumental support received from Analytical Science Division, CSMCRI, is gratefully acknowledged.

■ REFERENCES

(1) Service, R. F. *Science* **2006**, *313*, 1088−1090.
(2) Soroko, I.; Bhole, Y.; Livingston, A. G. *Green Chem.* **2011**, *13*, 162−168.
(3) Li, X.; Fustin, C.; Lefevre, N.; Gohy, J. F.; Feyter, S. D.; Baerdemaeker, J. D.; Egger, W.; Vankelecom, I. F. J. *J. Mater. Chem.* **2010**, *20*, 4333−4339.
(4) Bhattacharya, A; Ghosh, P. *Rev. Chem. Eng.* **2004**, *20*, 111−173.
(5) Beginn, U.; Zipp, G.; Mourran, A.; Walther, P.; Moller, M. *Adv. Mater.* **2000**, *12*, 513−516.
(6) Yang, S. Y.; Ryu, I.; Kim, H. Y.; Kim, J. K.; Jang, S. K.; Rusell, T. P. *Adv. Mater.* **2006**, *18*, 709−712.
(7) Akthuakul, A.; Salinara, R. F.; Myes, A. M. *Macromolecules* **2004**, *37*, 7663−7668.
(8) Sanchez, C.; Julian, B.; Belleville, P.; Popall, M. *J. Mater. Chem.* **2005**, *15*, 3559−3592.
(9) Kang, G. D.; Gao, C. J.; Chen, W. D.; Jie, X. M.; Cao, Y. M.; Yuan, Q. *J. Membr. Sci.* **2007**, *300*, 165−171.
(10) Park, H. B.; Freeman, B. D.; Zhang, Z. B.; Sankir, M.; McGrath, J. E. *Angew. Chem., Int. Ed.* **2008**, *47*, 6019−6024.
(11) Reese, E. T.; Mandels, M. *Cellulose and Cellulose Derivative Part V*; Bikales, N.M.; Segal, L., Eds.; Wiley-Interscience, NewYork, 1971; pp 1079.
(12) Allegrezza, A. E.; Parekh, B. S.; Parise, P. L.; Swiniarski, E. J.; White, J. L. *Desalination* **1987**, *64*, 285−304.
(13) Mansouri, J.; Harrisson, S.; Chen, V. *J. Mater. Chem.* **2010**, *20*, 4567−4586.
(14) Neo, Q. J. U.S. Patent US2007/0251883, 1−14, 2007.
(15) Koo, J. Y.; Hong, S. P.; Lee, J. H.; Ryu K. Y. U.S. Patent *US20070175821*, 1−9, 2007.
(16) Krishnan, S.; Weinman, C. J.; Ober, C. K. *J. Mater. Chem.* **2008**, *18*, 3405−3413.
(17) Louie, J. S.; Pinnau, I.; Ciobanu, I.; Ishida, K. P.; Ng, A.; Reinhard, M. *J. Membr. Sci.* **2006**, *280*, 762−770.
(18) Niu, Q. J.; Mickols, W. A.; Zhang, C.; US Patent *US20080185332*, 1−12, 2008.
(19) Colquhoun, H. M.; Chappell, D.; Lewis, A. L.; Lewis, D. F.; Finlan, G. T.; Williams, P. J. *J. Mater. Chem.* **2010**, *20*, 4629−4634.
(20) Liu, M.; Chen, Z.; Yu, S.; Wu, D.; Gao, C. *Desalination* **2011**, *270*, 248−257.
(21) Wei, X.; Wang, Z.; Chen, J.; Wang, J.; Wang, S. *J. Membr. Sci.* **2010**, *346*, 152−162.
(22) Schneider, R. P.; Ferreira, L. M.; Binder, P.; Bejarano, E. M.; Góes, K. P.; Slongo, E.; Machado, C. R.; Rosa, G. M. Z. *J. Membr. Sci.* **2005**, *266*, 18−29.
(23) Horii; Kannan, K. *Arch. Environ. Contam. Toxicol.* **2008**, *55*, 701−710.
(24) Suzuki, N.; Kiba, S.; Kamachi, Y.; Miyamotoc, N.; Yamauchi, Y. *J. Mater. Chem.* **2011**, *21*, 5338−5344.
(25) Egli, S.; Nussbaumer, M. G.; Balasubramanian, V.; Chami, M.; Bruns, N.; Palivan, C.; Meier, W. *J. Am. Chem. Soc.* **2011**, *133*, 4476−4483.
(26) Kim, J. W.; Kim, L. U.; Kim, C. K. *Biomacromolecules* **2007**, *8*, 215−222.
(27) Kugel, A.; Chisholm, B.; Ebert, S.; Jepperson, M.; Jarabek, L.; Stafslien, S. *Poly. Chem.* **2010**, *1*, 442−452.
(28) Sanchez, C.; Julian, B.; Belleville, P.; Popall, M. *J. Mater. Chem.* **2005**, *15*, 3559−3592.
(29) Zou, H.; Wu, S.; Shen, J. *Chem. Rev.* **2008**, *108*, 3893−3957.
(30) Tripathi, B. P.; Shahi, V. K. *Prog. Polym. Sci.* **2011**, *36*, 945−979.
(31) Suresh Kumar, G. V.; Rajendraprasad, Y.; Mallikarjuna, B. P.; Chandrashekar, S. M.; Kistayya, C. *Eur. J. Med. Chem.* **2010**, *45*, 2063−2074.

(32) Singh, A.; Singh, P.; Mishra, S. *J. Mater. Chem.* **2012**, *22*, 1834−1844.
(33) Singh, S.; Jasti, A.; Kumar, M.; Shahi, V. K. *Polym. Chem.* **2010**, *1*, 1302−1315.
(34) Tripathi, B. P.; Saxena, A.; Shahi, V. K. *J. Membr. Sci.* **2008**, *318*, 288−297.
(35) Zhou, M.; Nemade, P. R.; Lu, X.; Zeng, X.; Hatakeyama, E. S.; Noble, R. D.; Gin, D. L. *J. Am. Chem. Soc.* **2007**, *129*, 9574−9575.
(36) Singh, S.; Khulbe, K. C.; Matsuura, T.; Ramamurthy, P. *J. Membr. Sci.* **1998**, *142*, 111−127.
(37) Sambhy, V.; MacBride, M. M.; Peterson, B. R.; Sen, A. *J. Am. Chem. Soc.* **2006**, *128*, 9798−9808.
(38) Gomes, D.; Roeder, J.; Ponce, M. L.; Nunes, S. P. *J. Membr. Sci.* **2007**, *295*, 121−129.
(39) Socrates, G.; *Infrared Characteristic Group Frequencies*; Wiley: New York, 1980.
(40) Rorema, N. C. F.; Indelicato, J. *Water Res.* **2005**, *39*, 2731−2737.
(41) Kumar, M.; Singh, S.; Shahi, V. K. *J. Phys. Chem. B* **2010**, *114*, 198−206.
(42) Aimar, P.; Meireles, M.; Sanchez, V. *J. Membr. Sci.* **1990**, *54*, 321−338.
(43) Bowen, W. R.; Mohammad, A. W.; Hilal, N. *J. Membr. Sci.* **1997**, *126*, 91−105.
(44) Nightingale, E. R. Jr. *J. Phy. Chem.* **1959**, *63*, 1381−1387.
(45) Zhao, Y. H.; Zhu, X. Y.; Wee, K. H.; Bai, R. *J. Phys. Chem. B* **2010**, *114*, 2422−2429.
(46) Norberg, D.; Hong, S.; Taylor, J.; Zhao, Y. *Desalination* **2007**, *202*, 45−52.
(47) Ji, Y.; Anb, Q.; Zhaob, Q.; Chena, H.; Gao, C. *J. Membr. Sci.* **2011**, *376*, 254−265.
(48) Wei, X. Z.; Zhu, L. P.; Deng, H. Y.; Xu, Y. Y.; Zhu, B. K.; Huang, Z. M. *J. Membr. Sci.* **2008**, *323*, 278−287.
(49) Xu, T. W.; Yang, W. H. *J. Membr. Sci.* **2003**, *215*, 25−32.
(50) Ji, Y.; An, Q.; Zhao, Q.; Chen, H.; Qian, J.; Gao, C. *J. Membr. Sci.* **2010**, *357*, 80−89.
(51) Chojnowski, J.; Fortuniak, W.; Rościszewski, P.; Werel, W.; Łukasiak, J. *J. Inorg. Organomet. Polym. Mater.* **2006**, *16*, 219−230.
(52) Ortega, P.; Cobaleda, B. M.;´andez-Ros, J. M. H.; Paniagua, E. F.; Nieves, J. S.; Tarazona, M. P.; Copa-Patīno, J. L.; Soliveri, J.; Ǵomez, F. J. d. l. M. R. *Org. Biomol. Chem.* **2011**, *9*, 5238−5248.